Photodegradation of tartrazine dye favored by natural sunlight on pure and (Ce, Ag) co-doped ZnO catalysts

Tayeb Bouarroudj, Lamine Aoudjit, Lerari Djahida, Beddiaf Zaidi, Maamar Ouraghi, Djamila Zioui, Sarah Mahidine, Chander Shekhar and Khaldoun Bachari

ABSTRACT

In this work, the synthesis of pure and (Ce, Ag) co-doped ZnO was successfully accomplished using a solvothermal process. The synthesized samples were characterized by ultraviolet–visible spectroscopy, X-ray diffraction, and scanning electron microscopy. The photocatalytic ability of the samples is estimated through degradation of tartrazine in aqueous solution under photocatalytic conditions. The degradation study carried out for a reaction period of 90 min at and a free pH = 6.0 found that dye degradation is 44.82% for pure ZnO and 98.91% for (Ce, Ag) co-doped ZnO samples, indicating its excellent photocatalytic ability. Tartrazine mineralization was also studied by calculating the degradation of chemical oxygen demand. The effect of operating parameters such as catalyst dose, initial concentration of tartrazine, initial reaction pH, and nature of light source has been optimized for tartrazine degradation as a function of time. The reusability of ZnO and (Ce, Ag) co-doped ZnO catalysts was studied and its photocatalytic efficiency was found to be unchanged, even after six cycles of use. The mechanism of photocatalytic activity was also proposed.

Key words | azo dye, co-doped ZnO, degradation mechanism, photocatalysis, tartrazine, ZnO

HIGHLIGHTS

- The (Ce, Ag)/ZnO catalyst exhibited outstanding photocatalytic activity.
- The effect of tartrazine concentration on photocatalysis performance was studied.
- The degradation time of tartrazine using (Ce, Ag)/ZnO catalyst is 90 min.
- The reusability of our catalysts ZnO and (Ce, Ag)/ZnO was also explored.

Tayeb Bouarroudj (corresponding author)
Lerari Djahida
Maamar Ouraghi
Khaldoun Bachari
Centre de Recherche Scientifique et Technique en Analyses Physico-Chimiques (CRAPC),
BP384, Bou-Ismail,
RP42004 Tipaza,
Algeria
E-mail: *bouarroudj.tayeb@gmail.com*

Tayeb Bouarroudj
Centre de Recherche en Environnement (CRE),
BP 2024, Sidi Amar,
RP 23005, Annaba,
Algeria

Lamine Aoudjit
Djamila Zioui
Sarah Mahidine
Unité de Développement des Équipements Solaires, UDES/Centre de Développement des Energies Renouvelables, CDER,
Bou-Ismail,
42415 W. Tipaza,
Algeria

Beddiaf Zaidi
Department of Physics, Faculty of Matter Sciences,
University of Batna 1,
Batna,
Algeria

Chander Shekhar
Department of Physics, Amity School of Applied Sciences,
Amity University Gurgaon,
Haryana 122413,
India

doi: 10.2166/wst.2021.106

GRAPHICAL ABSTRACT

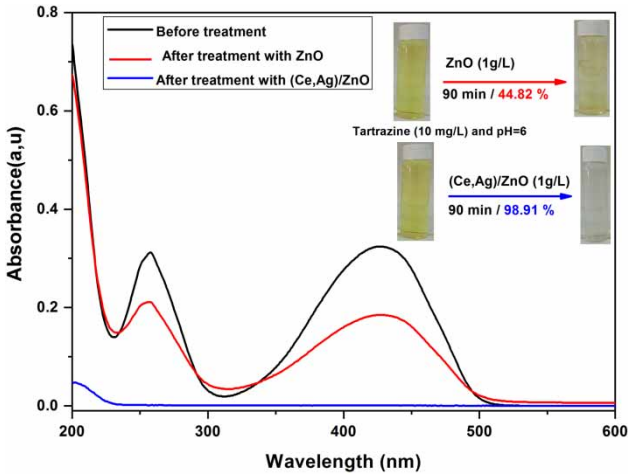

INTRODUCTION

Growing consumption coupled with the increasingly declining supplies of water has driven society and governments to consider the decontamination of contaminated water as the source of the usable water for selected household, industrial, and agriculture usage. The decontamination of wastewater using advanced oxidation processes (AOP) (Oller *et al.* 2011), phytoremediation (Salt *et al.* 1998), photocatalysts (Herrmann *et al.* 1993), electrochemical techniques (Brillas & Martínez-Huitle 2015), biosorption (Vieira & Volesky 2000), and nanotechnology (Baruah *et al.* 2015) has been reported as possible techniques for wastewater purification and solar wastewater treatment (SOWAT) (Igoud *et al.* 2020). Many scientists, industrialists, and policymakers have collaborated to develop materials and technology for a safe world with the intention of successfully eliminating dye effluents (Salthammer *et al.* 2010; Vaiano *et al.* 2016). The majority of water contaminants are residual colors found in the effluents from various industries, e.g. paper and pulp, textile, dye, pharmaceutical, cosmetics, rubber, paints, and printing industries, etc. (Ali *et al.* 2018a). Discharge of pollutants from these industries into water sources poses a major environmental threat across the world. Not only do pollutants harm the esthetic quality of water, but they also destroy marine flora and fauna (Kaur & Singhal 2014). Tartrazine (C.I. Acid Yellow 23, AY23) is chosen for the present research as a model pollutant for such dyes an dius called by other names including E102 (EFSA), FD&C Yellow 5 (FDA-US Food and Drug Administration, FDA) or C.I. 19140 (Color Index International). It is approved as a dye by the FDA (Bhatt *et al.* 2018) and is a widely used azoic dye in the textile, cosmetics, medicinal, and food industries (Aoudjit *et al.* 2018). Many studies have been published on tartrazine hazards in recent times, describing its potentially deleterious impact, such as food allergy, mutagenic, carcinogenic, and phototoxicity (Abdullah Hashim *et al.* 2001; dos Santos *et al.* 2014; Chekir *et al.* 2017; Aoudjit *et al.* 2018; Ali *et al.* 2018b).

Tartrazine's chemical name is trisodium-5 hydroxy-1-(4-sulfonatophenyl)-4-(4-sulfonatophenylazo)-H-pyrazole-3-carboxylate and incorporates azo bonding (–N = N–) in its form, believed to be metabolized by intestinal bacteria into sulfanilic acid and aminopyrazolone (Rehman *et al.* 2019). The chemical structure of the tartrazine is presented in Figure 1.

Advanced oxidation processes (AOPs have been defined in recent years as effective procedures for obtaining high oxidation yields from several types of organic compounds.

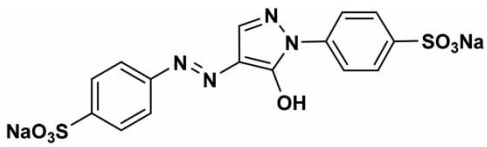

Figure 1 | Chemical structure of tartrazine.

These approaches are focused on the production of very reactive agents such as hydroxyl radicals (OH) that are highly reactive and fast oxidizing agents ($E^o = 2.8$ V), capable of mineralizing organic contaminants (Daneshvar *et al.* 2005; Saien & Soleymani 2007). Semiconductors based on metal oxides have been widely developed in recent decades for photocatalytic applications (Guo *et al.* 2011; Kamegawa *et al.* 2011, 2012; Chen *et al.* 2017). The photocatalysts may capture photons with energy equal to or greater than their band gap energy during the photocatalytic phase to form electrons and holes on the catalyst surface. It is known that superoxide and hydroxyl radicals are generated to oxidize organic contaminants by interacting between holes or electrons and water molecules (Fu *et al.* 2015). The photocatalysts in the spectral region can be classified into two standardized classes according to their different photocatalytic properties: ultraviolet (UV) and visible light-responsive photocatalysts (Su *et al.* 2019). Among the various semiconductors, zinc oxide (ZnO) is a photocatalyst with a large direct band gap (3.3 eV) and has a high binding free-excision capacity of 60 meV (Nair *et al.* 2011). Because of these characteristics, ZnO is regarded as one of the main active photocatalysts, including high initial operation levels, multiple active sites with high surface reactivity, low price, and environmental protection (Lam *et al.* 2012). Different strategies were therefore adopted to enhance photocatalytic activity of ZnO. Doping is well known to be an effective and easy way of improving the photocatalytic properties. Surface area variability and dopant ion incorporation produce lattice defects and band gap energy transition (Ullah & Dutta 2008; Kao *et al.* 2011), which play an important role in metal oxides photocatalytic operations. Doping transition metals, noble metals, and non-metals is therefore a very expedient way to improve the photocatalytic activity (Poongodi *et al.* 2015). Modification of noble metal semiconductors has gained tremendous interest because they improve the reduction cycle and hence the mechanism of photocatalytic degradation. Silver (Ag) was selected among the noble metals because of its extraordinary catalytic ability, non-toxicity, and comparatively cost-effectiveness. Ag can trap the photogenerated electrons from the semiconductor and allow holes to form hydroxyl radicals, which results in the degradation reaction of the present organic species (Saravanan *et al.* 2013).

Rare earth (RE) metals are also strong doping elements for modifying ZnO's electronic structure and extending its visible light absorption. Doping with RE metals is a localized level of impurity in ZnO's band structure, and changes the band structure (Khatamian *et al.* 2012). Cerium (Ce) has received considerable attention from various lanthanides as a promising dopant for semiconducting metal oxide materials due to several unique properties and applications (Chang *et al.* 2014; Lamba *et al.* 2015; Li *et al.* 2015). Ce doping has been found to increase the efficiency of ZnO in photocatalytic applications. Ce doping facilitates the formation of crystallite to minimize particle size and increase the surface area, thereby helping to improve the efficiency of photodegradation (Rezaei & Habibi-Yangjeh 2013). Recently, simultaneous doping into semiconductor materials with two groups of atoms (co-doping) has drawn significant interest, as it may contribute to higher photocatalytic behavior and different characteristics relative to single element doping into semiconductor oxides (Zhao *et al.* 2011).

In this work, in conjunction with ZnO and (Ce, Ag) co-doped ZnO catalysts, solar-light irradiation has been successfully used to efficiently remove tartrazine from polluted water. The remediation of dyes in effluents employs methods such as electrochemical treatment, membrane filtration, adsorption, and hybrid technologies, among others. However, these technologies lack efficiency and cost-effectiveness. As a possible solution, this work presents a photodegradation of tartrazine dye favored by natural sunlight on pure and (Ce, Ag) co-doped ZnO catalysts.

MATERIALS AND METHODS

Chemical reagents

Tartrazine ($M = 534.36$ g/mol, assay: $\geq$85%) also known as Yellow 23 (Figure 1), with the chemical formula $C_{16}H_9N_4Na_3O_9S_2$ and a maximum absorption at the wavelength at 427 nm was purchased from ACROS organics (USA). Hydrochloric acid (HCl) and sodium hydroxide (NaOH) used in this study were laboratory grade products. Deionized water was used for all experiments.

Materials

A 100 mL borosilicate glass Erlenmeyer flask was used as the reactor. Global solar radiation intensity was measured with a Kipp and Zonen CMP11 pyranometer, pH value was measured using CONSORT C3010 multi-parameter analyzer, tartrazine dye concentration was determined using Shimadzu UV1800 Spectrophotometer and chemical oxygen demand (COD) was measured by type (DR 1900 LANGE HACH, Düsseldorf, Germany) spectrophotometer.

The experiments were performed using solar irradiation at Bou-Ismail, Algeria, during April 2020 between 10:00 and 16:00 at the Solar Equipment Development Unit, situated 30 km west of Algiers (longitude: 2 W 420 N, latitude: 36 W 390 E, altitude: 5 m). The entire system is linked to photovoltaic panels providing energy for the alimentation (agitation) of our system for degradation of tartrazine.

EXPERIMENTAL

Catalysts preparation

A sufficient quantity of $Zn(NO_3)_2{\cdot}4H_2O$ was dissolved in bi-distilled water. The pH of the solution was brought to 7.5 by drop-wise addition of ammonium hydroxide solution (25%). The reaction mixture was then stirred for 2 h at room temperature with 100 rpm and transferred to a steel autoclave coated with Teflon and kept at 120 °C for 22 h. The product was washed several times using a vacuum filtration unit with bi-distilled water, filtered and dried at 80 °C overnight. The co-doped ZnO nanoparticles (heterojunction) were also prepared according to the same procedure, except that the products of cerium chlorides and silver nitrates ($CeCl_3$ and $AgNO_3$) were added.

Catalysts characterization

The X-ray diffraction (XRD) patterns and scanning electron microscope (SEM) micrographs of the samples prepared as mentioned above were recorded. The XRD patterns were recorded on a Siemens D-5000 diffractometer with Cu-Kα radiation ($\lambda = 1.5418$ Å) and surface morphology was studied using SEM. The UV–Vis absorption spectra were measured by UV–Vis spectrophotometer (Shimadzu UV-2401).

Photocatalytic degradation of tartrazine

Photocatalytic process was conducted through batch mode at room temperature using the setup as shown in Figure 2. Dye solutions of desired concentrations (10, 20, and 30 mg/L) were prepared by dissolving the corresponding amount of tartrazine in distilled water. The concentrations of the dye solution have been selected as per the concentration given in the literature (Tassalit *et al.* 2016; Aoudjit *et al.* 2017; Chekir *et al.* 2017).

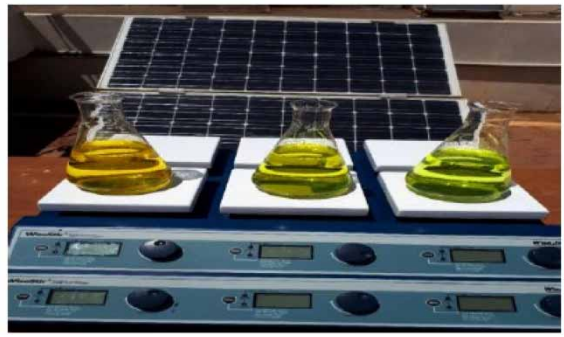

Figure 2 | Schematic representation of the experimental setup used for tartrazine degradation assays under sunlight radiation.

The optimal catalyst dose of 1 g/L at 15 min time intervals was used for extraction of the sample in the present study. The pH of the solution was adjusted by the addition of NaOH or HCl to the solution. To carry out the photochemical reaction, an appropriate amount of ZnO and (Ce, Ag) co-doped ZnO (1 g/L) was added to tartrazine solutions in a magnetic stirrer. Each sample was kept in the dark for 20 min. After ensuring the adsorption equilibrium, the reactor was exposed to the sunlight for 2 h. Thereafter, 3 mL aliquot of tartrazine solution was withdrawn from the reaction mixture at 15 min time intervals and filtered with a Millipore membrane with a pore size = 0.45 μm prior the analysis to the separation of the catalyst. This is followed by measurement of absorbance of the solution at 427 nm by UV–Vis spectrophotometer. The percentage of degradation was estimated using the following equation

$$\text{Degradation (\%)} = \frac{C_0 - C_t}{C_0} \times 100 \quad (1)$$

where C_0 is the initial dye concentration and C_t is the tartrazine concentration at certain reaction time t (min).

COD measurements

In order to assess the mineralization rate of the tartrazine under the optimum condition free pH = 6.0 of the solution, 1 g/L dose of catalysts was used. The tartrazine concentration $C_{TART} = 10$ mg/L and solar ultraviolet radiation (853 W/m^2) was used. The samples were taken from the beginning and end of the reaction and analyzed by COD based on the oxidation of organic materials by an excess of potassium dichromate ($K_2Cr_2O_7$), in acidic medium and

boiling, in the presence of silver sulfate (Ag_2SO_4) and mercury sulfate ($HgSO_4$). The COD abatement rate given in percentage (%) is calculated by the following equation as given by (Zioui *et al.* 2019):

$$\text{COD}\,(\%) = \frac{\text{COD}_0 - \text{COD}_t}{\text{COD}_0} \times 100, \quad (2)$$

where COD_0 and COD_t are the initial COD and COD at time t, respectively.

RESULTS AND DISCUSSION

Characterization of catalyst

XRD

XRD analysis of samples was carried out to determine the crystal structures and phase purities of ZnO and (Ce, Ag)/ZnO. The XRD patterns are shown in Figure 3. The main diffraction peaks for pure ZnO were observed at 2θ values of 31.73, 34.37, 36.21, 47.48, 56.53, 62.77, 66.30, 67.86, 69.00, 72.46, and 76.86 corresponding to the lattice plane (100), (002), (101), (102), (110), (103), (200), (212), (201), (004), and (202)planes of wurtzite ZnO hexagonal phase (space group, P63mc), which are in good agreement with the literature values (PDF 89-1397) (Kumar *et al.* 2015).

For (Ce, Ag)/ZnO, diffraction peaks well suited to (100), (002), (101), (102), (110), (103), (200), (212), (201), (004), and (202) planes at 2θ values were same as that of wurtzite ZnO hexagonal phase. There were additional diffraction peaks observed corresponding to the Ag and CeO_2. The diffraction peaks at 2θ values 38.11, 44.30, 64.44, and 77.39, labeled with '◊' matched with the (111), (200), (220), and (311) crystalline planes of cubic phase (space group, Fm-3 m) of metallic Ag (PDF 65-2871) (Güy & Özacar 2019), and the diffraction peaks at 2θ values 27.79, 32.20, 46.18, and 56.09, marked with '*' matched with the (222), (400), (440), and (631) planes of cubic phase (Ia-3) of CeO_2 (PDF 89-8429) (Wen *et al.* 2018). XRD analysis therefore suggests that the wurtzite ZnO hexagonal phase is present in the pure ZnO samples and in the (Ag, Ce) co-doped samples, wurtzite ZnO hexagonal phase along with the metallic Ag in cubic phase, and CeO_2 in cubic phase is also present.

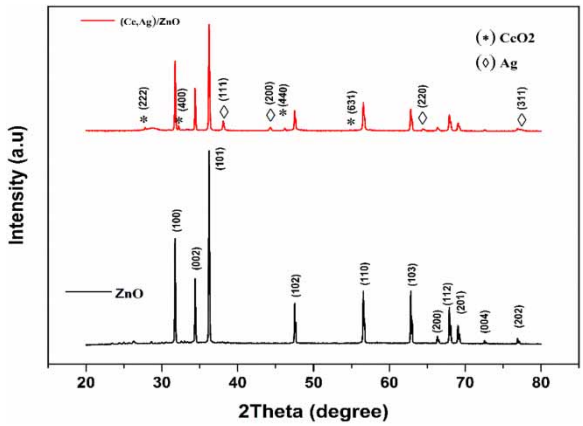

Figure 3 | XRD patterns of ZnO and (Ce, Ag) co-doped ZnO.

SEM analysis

The surface morphology of the samples was obtained by SEM and is presented in Figure 4. From Figure 4(a) and 4(b), hexagonal rods of ZnO and (Ce, Ag) co-doped ZnO catalysts can be observed. However, the average size of the crystallites in the pure ZnO sample is considerably larger compared to the average size in the (Ce, Ag) co-doped ZnO sample. The decrease in crystallite size with the co-doping of Ce and Ag leads to an increase in the specific surface area compared to the undoped samples. Additionally, the surface of (Ce, Ag) co-doped ZnO samples have numerous fibrous columns anchored from the ZnO surface, which is conducive to forming the heterojunction between ZnO and (Ce, Ag) dopants. The presence of such fibrous columns on the ZnO surface increases the total surface area of co-doped samples, and therefore increases the catalytic performance of the samples immensely.

Optical proprieties

Figure 5(a) shows the UV-Vis absorption spectra of the ZnO and (Ce, Ag)/ZnO. Interestingly, with the Ag and Ce co-doping, the absorption peak changes from 283 to 352 nm. This change in the absorption peak to the higher wavelength results in the decrease of band gap of (Ce, Ag)/ZnO. A single absorption peak for (Ce, Ag)/ZnO shows that Ce and Ag are doped effectively into ZnO lattices and that the sample has strong optical properties (Kumar *et al.* 2015).

The optical band gap (Eg) of pure and (Ce, Ag) co-doped ZnO was calculated using the Tauc relationship (J. Tauc *et al.*):

$$(\alpha h\nu)2 = A(h\nu - Eg) \quad (3)$$

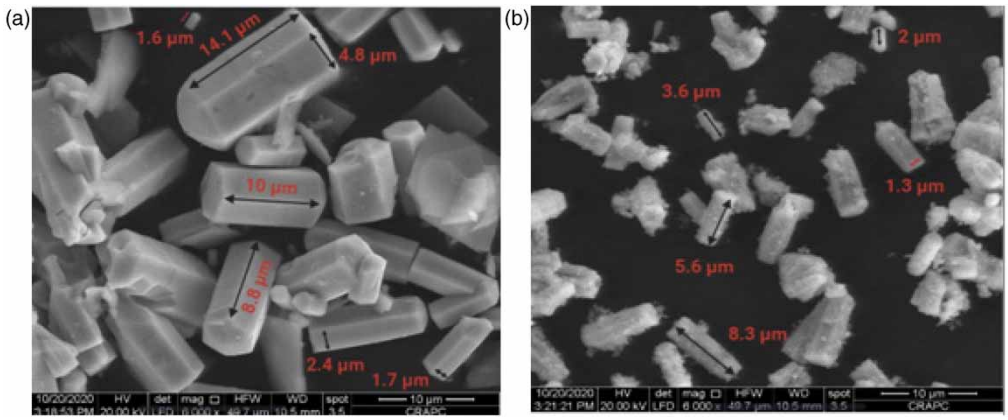

Figure 4 | (a) SEM micrograph of ZnO and (b) (Ce, Ag) co-doped ZnO.

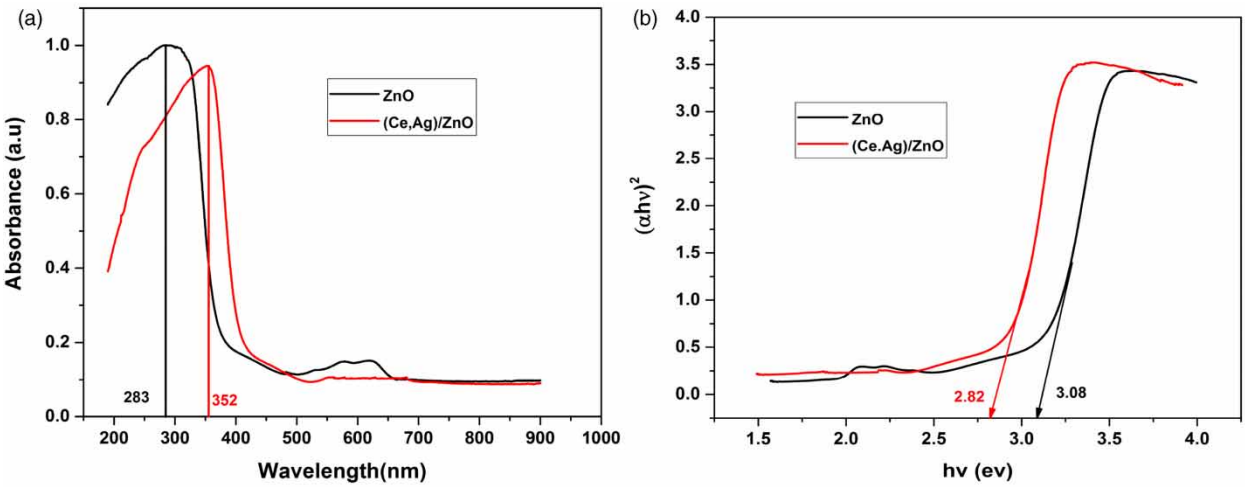

Figure 5 | (a) Optical absorbance spectra of ZnO and (Ce, Ag)/ZnO, (b) plot of $(\alpha h\nu)^2$ as a function of incident photon energy.

The Tauc plot to calculate the optical band gap of the samples is presented in Figure 5(b). The band gap is determined by extrapolating the linear portion of the plot between $(\alpha h\nu)^2$ and hv to intersect the x-axis. The value of the optical band gap energy of the pure and (Ce, Ag) co-doped ZnO samples decreases from 3.08 to 2.82 eV, respectively. The decrease in the band gap of the semiconductor is due to the additional impurity levels generated in the doped samples. The band gap energy value was decreased for the (Ce, Ag)/ZnO samples. This result reveals that the co-doped ZnO absorbs UV and visible light. Therefore, the optical absorption property attributes that the (Ce, Ag)/ZnO photocatalyst could be promising in visible light photocatalysis (Poongodi *et al.* 2015).

PHOTODEGRADATION OF TARTRAZINE

Evaluation of treatment method on the degradation of tartrazine

Preliminary experiments were carried out to determine the photocatalysis performance. Three main removal procedures were tested during our analysis for the efficacy of tartrazine degradation in polluted water. The first procedure was carried out in the presence of catalyst without radiation based on the adsorption; the second procedure was performed in the presence of solar radiation without catalyst based on the photolysis; the third procedure was carried out under solar radiation (with sunlight) and in the presence of catalyst based on photocatalysis.

Degradation of tartrazine under these processes for pure ZnO and (Ce-Ag) co-doped ZnO is presented in Figure 6. It can be observed that photocatalysis is impactful in photodegradation of tartrazine, whereas the effect of adsorption and photolysis is negligible. These results are in good agreement with similar works (Tanaka *et al.* 2000; Chekir *et al.* 2017; Aoudjit *et al.* 2018). In our azo dye degradation studies, the degradation of tartrazine under photocatalytic conditions in the presence of pure ZnO catalysts for a reaction time of 90 min is 44.82% and 98.91% for (Ce-Ag) co-doped ZnO. The degradation in presence of ZnO increases rapidly for 30 min until it reaches 24%. Thereafter, it slows down for 90 min until reaching 44.82%. For (Ce–Ag) co-doped ZnO, the degradation of the azo dye saturates in about 45 min to ~95% and takes almost 90 min for 100% degradation. However, during photolysis or adsorption, no signs of removal were observed, as indicated in Figure 6. Further investigations and refinement of different process parameters and optimal conditions used for the effective extraction of tartrazine from polluted water were taken.

Effect of radiation source

The effect of irradiation type on the photocatalytic degradation of tartrazine by ZnO and (Ce, Ag) co-doped ZnO was studied by artificial irradiation (PHILPS PL-L 24 W/10/4P UV lamps, $\lambda_{max} = 365$ nm and $I = 18.6$ W/m^2), and solar UV radiation using a global UV radiometer (Kipp & Zonzn, CMP11, $I = 853$ W/m^2). As seen in Figure 7(b), after 90 min of exposure, the degradation percentage of tartrazine due to (Ce, Ag) co-doped ZnO photocatalysts was 98.91%, and 98.88%, under sunlight and UV lamp, respectively. The corresponding values for the degradation of the tartrazine due to ZnO are found to be 42.02% and 13.79%, respectively, as shown in Figure 7(a). Comparison of the photocatalytic efficiency ZnO and (Ce, Ag) co-doped ZnO irradiated with the sunlight and UV radiation under identical experimental condition is presented in Figure 8. These results indicate a remarkable photocatalytic activity of (Ce, Ag) co-doped ZnO photocatalyst. The possible mechanism for the degradation efficiency of the photocatalyst is presented as follows: upon absorption of light by the photocatalyst, the electrons from the valence band are transferred to the conduction band, along with the production of holes in the valence band. The photo-created electrons reduce the oxygen to form superoxide radicals (O^{2-}) and at the same time holes present in the valence band oxidize the water molecules/OH^- ions to produce hydroxyl radicals ($OH^{\cdot}$). These superoxide and hydroxyl radicals participate in the degradation process of tartrazine dye. It was previously observed that photogenerated electrons that move to the conduction band are mostly unstable and quickly go back to the valence band. Therefore, they can recombine with the holes by going to the valence band and decrease the quantum efficiency of photocatalysis. In this study, enhancement in photocatalytic performance of (Ag, Ce) co-doped ZnO can be attributed to the combined effect of Ag and Ce co-doping. The localized electronic states of dopant ions (Ag^+,Ce^{3+}) may be acting as charge trap sites for photo-created electron-hole pairs (Khalid *et al.* 2019).

The use of natural sunlight, instead of the artificial UV lamp, may help greatly in reducing the cost of photocatalytic oxidation compared to some alternative technologies. The availability of solar UV-irradiation at a specific geographical

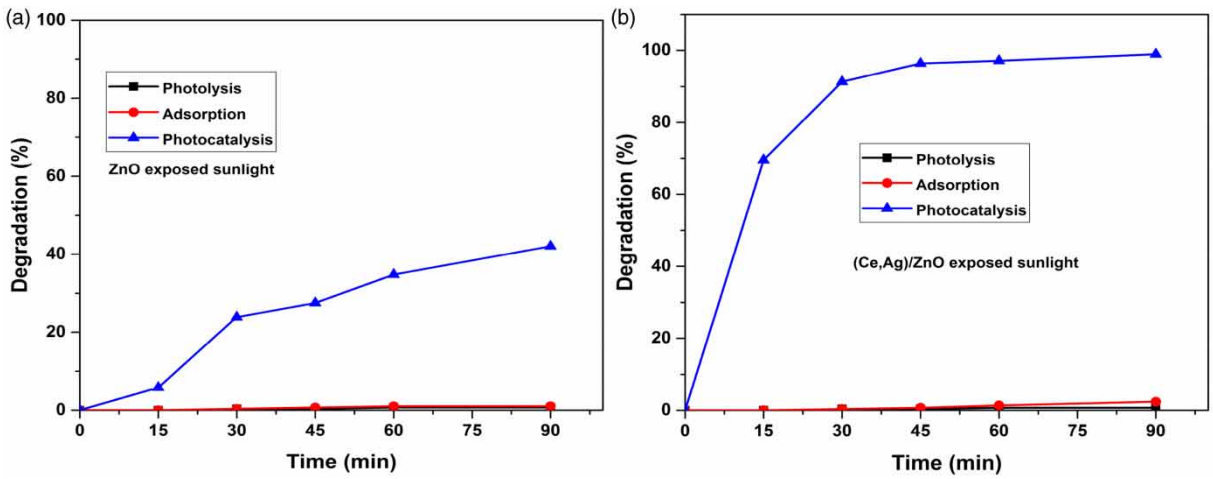

Figure 6 | Degradation of tartrazine under different processes ($C_{TART} = 10$ mg/L, $C_{catalyst} = 1$ g/L, and pH = 6). (a) For ZnO and (b) for (Ce, Ag) co-doped ZnO under solar radiation.

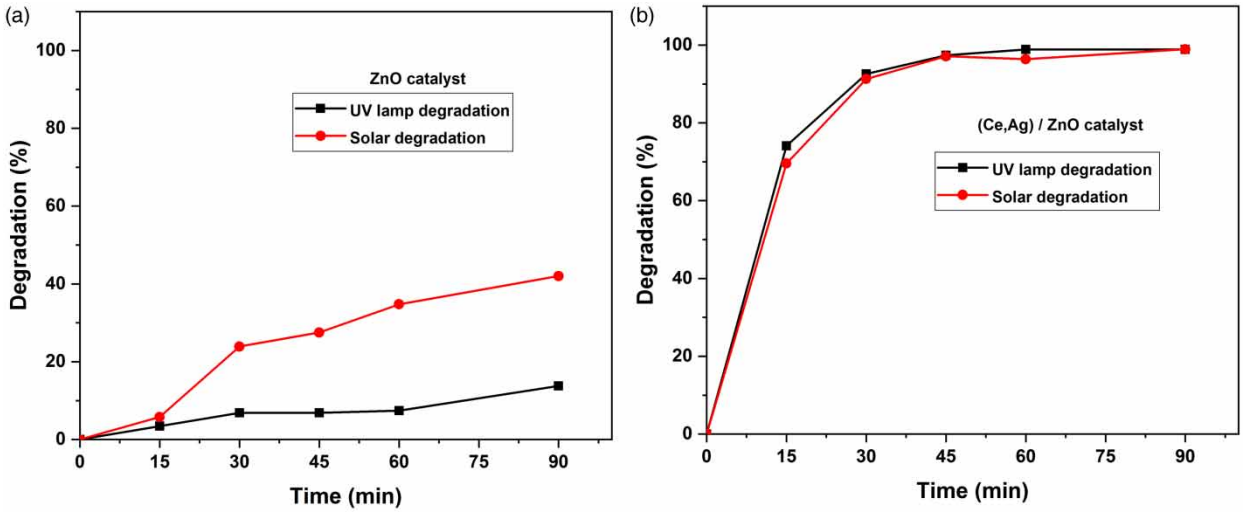

Figure 7 | Degradation of tartrazine exposed to different sources of light (C_{TART} = 10 mg/L, $C_{catalyst}$ = 1 g/L, and pH = 6. (a) For (Ce, Ag) co-doped ZnO and (b) for ZnO.

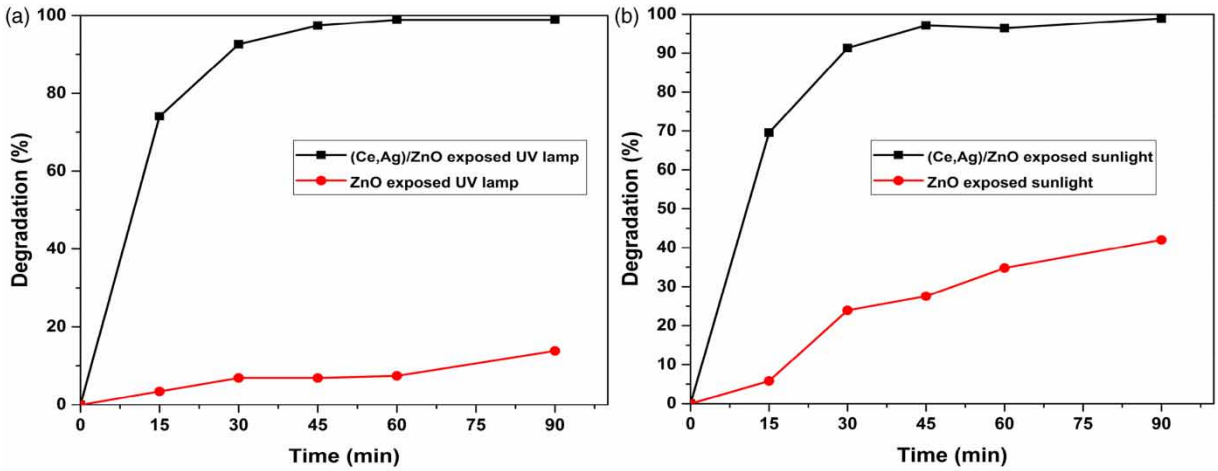

Figure 8 | Comparison of degradation of tartrazine exposed to different sources of light (C_{TART} = 10 mg/L, and catalyst = 1 g/L). (a) Sunlight irradiation and (b) UV lamp irradiation.

area, like Algeria, represents a major factor in determining the cost of a solar-based system. Algeria is characterized by an important solar potential and an annual duration of sunshine exceeding (3,000 h/y). Solar photocatalysis can be recommended for its low-cost energy and high efficiency. These results are in good agreement with similar works reported in the literature (Aoudjit *et al.* 2018; Zioui *et al.* 2019; Ghribi *et al.* 2020).

Effect of solution pH

Photodegradation is well known to be influenced by the adsorption of the dye on the catalyst surface. The dye's adsorption is strongly influenced by the pH of the solution (Velmurugan & Swaminathan 2011; Krishnakumar *et al.* 2012; Subash *et al.* 2013). Thus, in this study the effect of pH on tartrazine photodegradation was studied in an aqueous medium. The experiments were conducted at a concentration of 10 mg/L tartrazine to cover a $3.0 \leq pH \leq 9.0$ for 90 min of sunlight irradiation. The effect of the pH on the photodegradation of tartrazine in the presence of ZnO and (Ce, Ag)/ZnO exposed to the sunlight is presented in Figure 9. Looking at the Figure 9(a), it can be observed that the degradation of tartrazine molecule is very high in the presence of (Ce, Ag)/ZnO catalyst throughout the pH range. The degradation percentage of tartrazine increases almost linearly as a function of time at different pH values, with a maximum at pH = 9.0 as shown in Figure 8(b).

The interpretation of pH effects on dye photodegradation process output is a very challenging task due to its

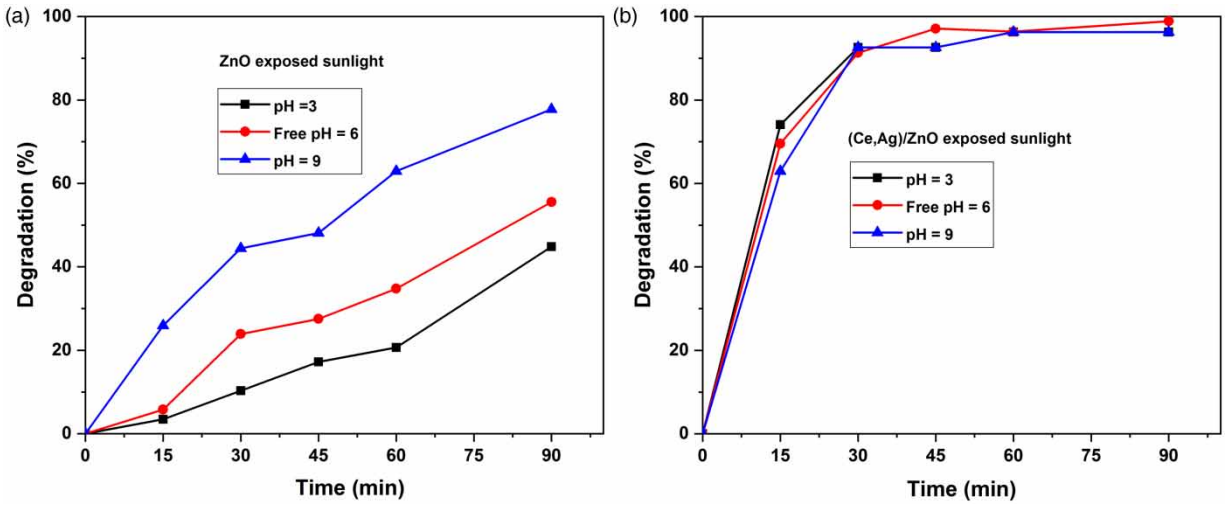

Figure 9 | Sunlight photodegradation of tartrazine at different pH (C_{TART} = 10 mg/L and catalyst = 1 g/L). (a) For (Ce, Ag) co-doped ZnO and (b) for ZnO.

dependence on various physical and chemical parameters. First, the influence of pH of the solution on the rate of degradation can be explained primarily by the processes of sorption–desorption in the semiconductor particle sheet (Chekir *et al.* 2017). The azo dye used in the present experiment was anionic dye, and under laboratory conditions was negatively charged. For this reason, it is best to use the solution's free pH. The photocatalytic degradation of tartrazine at free pH is 98.91% for (Ce, Ag) co-doped ZnO catalyst.

Effect of initial concentration of tartrazine

Figure 10 shows the effect of initial concentration of tartrazine on the rate of photodegradation at free pH = 6.0 for a reaction time of 90 min. The increase in the amount of tartrazine from 10 to 30 mg/L shows decreased degradation percentage, indicating slower degradation kinetics for ZnO catalyst in the presence of sunlight.

For the (Ce-Ag) co-doped ZnO catalyst, the degradation percentage decreases with an increase in the tartrazine concentration. With an increase in the concentration of tartrazine, the degradation behavior changes from initial rapid degradation at 10 mg/L to linear at 30 mg/L. After 90 min, 12% reduction in the degradation of the 30 mg/L tartrazine solution was observed. This could be because of insufficient quantity of generated $OH^{\cdot}$ radicals present in the solution, which influence the photodegradation process favorably (Li *et al.* 2010; Farzadkia *et al.* 2014; Tran *et al.* 2018). Degradation rate is proportional to the available surface of the catalyst for the development of electron-hole pairs to generate hydroxyl radicals. In the present study, for the constant

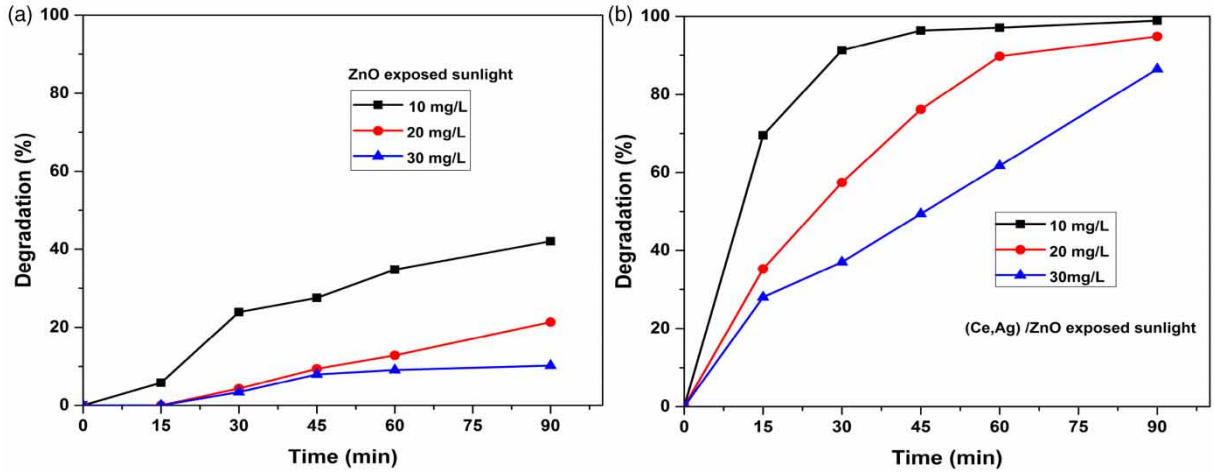

Figure 10 | Photodegradation of tartrazine with time at different concentrations in sunlight (free pH = 6 and catalyst = 1 g/L). (a) ZnO and (b) (Ce, Ag) co-doped ZnO.

volume of catalyst, the number of hydroxyl radicals produced remains the same, although the concentration of dye in the solution increases. Consequently, the ratio of hydroxyl radicals to tartrazine molecules decreases with the increase in dye concentration (Jamil & Sharaf El-Deen 2016). Additionally, the decrease in dye degradation has been attributed to a decrease in light penetration into the solution (Krishnakumar *et al.* 2012). The amount of the dye adsorbed on the catalytic surface increases with the increase in the dye concentration in solution. This higher particle density of the dye molecules in the solution reduces the penetration depth of incident photon in the dye solution. At high dye concentrations, the adsorbed dyemolecules absorb the majority of the incident visible light, effectively preventing the light reaching the catalyst. This shielding of the catalyst from the sunlight can therefore also decrease photocatalytic degradation (Davis *et al.* 1994).

Effect of photocatalysts dose

The influence of the catalyst dose on the tartrazine photodegradation is illustrated in Figure 11. The catalyst dose varies from 0.5 g/L to 2 g/L. The degradation increases with the increase in the dose and the maximum degradation occurs for an optimal dose of 1 g/L. This is due to increased availability of active sites on the photocatalyst surface and hydroxyl radicals ($OH^{\cdot}$) in the reaction mixture. However, a further increase of catalyst dose beyond 1 g/L decreases the catalytic degradation. In fact, an excess amount of catalyst could notably inhibit the penetration of solar light into the tartarazine solution, and an increase in the photocatalyst suspension leads to a decrease in the generation of oxidizing agents. Consequently, 1 g/L catalyst dose was chosen as the optimum dose for further experiments.

Recyclability of catalysts

The recyclability of ZnO and (Ce, Ag) co-doped ZnO (1 g/L) catalysts used in the photodegradation of tartrazine (C_{TART} = 10 mg/L) at free pH = 6.0 has also been studied under sunlight irradiation over the course of 90 min and the results are presented in Figure 12. To reuse the photocatalyst in multiple cycles, the photocatalyst was collected, washed with distilled water, dried, and then used in a new experimental cycle. After six cycles of treatment, the catalyst still maintained good photodegradation capacity. The degradation percentage of tartrazine during the six cycles were 98.91%, 98.89%, 98.36%, 97.86%, 97.36%, and 97.16% for (Ce, Ag) co-doped ZnO, as shown in Figure 12(b), and 42.02%, 42.02%, 40.86%, 40.30%, 39.87%, and 39.12% for ZnO as shown in Figure 12(a). This confirms the excellent reusability of (Ce, Ag) co-doped ZnO photocatalysts. The high degradation activity could be attributed to the highly stable nature of (Ce, Ag) co-doped ZnO, while its surface remained resistant to agglomeration or sintering under the experimental conditions specified.

Su *et al.* (2019) reported similar findings for ZnO/Ag–Ag_2O based catalyst on Congo Red degradation after five cycles. Subash *et al.* (2012) reported strong recyclability of catalysts when using Ce co-doped Ag–ZnO under natural sunlight

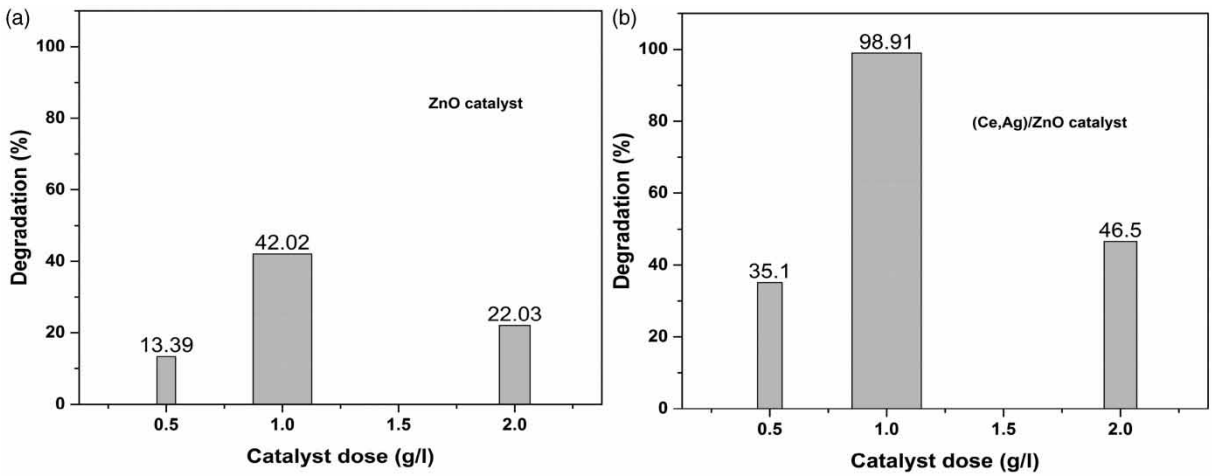

Figure 11 | Photodegradation of tartrazine at different concentration of catalyst in sunlight (free pH = 6 and C_{TART} = 10 mg/L). (a) ZnO and (b) (Ce, Ag) co-doped ZnO.

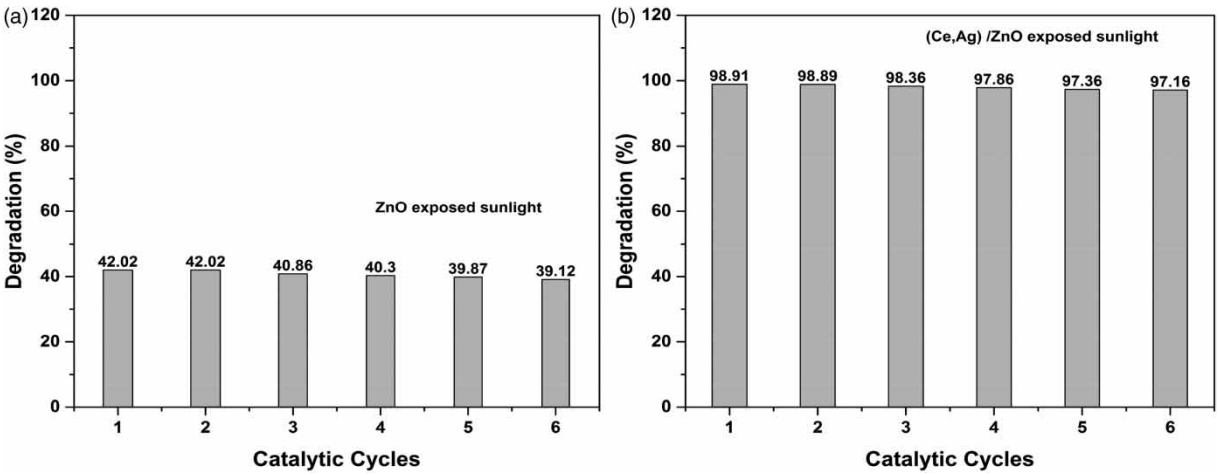

Figure 12 | Photodegradation of tartrazine over six catalytic cycles in sunlight (C_{TART} = 10 mg/L, $C_{catalyst}$ = 1 g/L and pH = 6). (a) ZnO and (b) (Ce, Ag) co-doped ZnO.

for Naphtol Blue Black dye photodegradation. In metronidazole photodegradation, Dong *et al.* (2014) reported strong recyclability of catalysts when using ZnO/reduced graphene oxide under visible light.

COD analysis

The degradation of the tartrazine was also analyzed using COD values to confirm the mineralization of tartrazine. All parameters of the reaction such as (tartrazine concentration (C_{TART} = 10 mg/L), solar UV radiation (853 W/m^2), dose of catalysts (1 g/L), and free pH = 6 conditions over the course of 90 min) were kept constant during the experiments.

Table 1 shows the percentage of COD reductions obtained in this study. After 90 min, the value of COD with pure ZnO and (Ce, Ag) co-doped ZnO irradiation was 30.39% and 78.43%, respectively, indicating the dye mineralization and the higher potential of (Ce, Ag) co-doped ZnO system for the removal of dyes from wastewater.

Table 1 | COD value for pure ZnO and (Ce, Ag) co-doped ZnO and respective removal rate (%) for tartrazine after degradation under sun irradiation

COD	Initial	Final	%
ZnO	102	71	30.39
(Ce, Ag)/ZnO	102	22	78.43

Kinetic analysis as a function of tartrazine concentration

The kinetics of photocatalytic degradation of tartrazine can be depicted using the first-order equation given by Equation (4) (Nezamzadeh-Ejhieh & Hushmandrad 2010; Aoudjit *et al.* 2020; Omrani & Nezamzadeh-Ejhieh 2020; Martins *et al.* 2021).

$$\ln\left(\frac{C_0}{C_t}\right) = K_{app}t \quad (4)$$

where K_{app} is the pseudo-first-order rate constant (min^{-1}), C_0 is the initial concentration; C_t is the concentration of tartrazine at time t (min). The estimated pseudo-first-order rate constant and corresponding R^2 values are presented in Table 2. With an increase in dye concentration from 10 to 30 mg/L, the degradation rate constant decreases from 0.006 to 0.001 min^{-1} in the case of ZnO and from 0.057 to 0.019 min^{-1} in the case of (Ce, Ag)/ZnO.

MECHANISM OF DEGRADATION

In general, photocatalytic degradation by semiconductors involves three steps: (1) irradiation of the semiconducting catalyst causes the transfer of electrons from the valence band (VB) to the conduction band (CB), creating equal number of empty sites (holes) in the valance band; (2) the excited electrons and holes then migrate to the catalyst surface; and (3) the excited electrons and holes react with free radicals such as OH^-, and O_2^- resulting in oxidation and reduction processes, respectively. Such free radicals further react with organic dye and degrade them in the process to components, harmless compounds such as CO_2, H_2O, and inorganic by-products (Beura & Thangadurai 2017; Kumar *et al.* 2019).

Table 2 | Effect of initial dye concentration (C_0) on photocatalytic degradation efficiency (%) and apparent reaction rate (K_{app}) of tartrazine

	ZnO catalyst			(Ce, Ag) co-doped ZnO catalyst		
C_0 (mg/L)	Degradation (%)	K_{app} (min^{-1})	R^2	Degradation (%)	K_{app} (min^{-1})	R^2
10	42.02	0.006	0.94	98.91	0.057	0.88
20	21.36	0.002	0.94	94.88	0.033	0.98
30	10.22	0.001	0.88	86.50	0.019	0.98

For pure ZnO catalyst

Various chemical reactions that produce reactive species during degradation of the photocatalytic dye can be summarized as follows (Tunesi & Anderson 1991; Zhao *et al.* 1998; Chen *et al.* 2005; Fujishima *et al.* 2008; Habba *et al.* 2016; Kumaran & Muraleedharan 2017; Ani *et al.* 2018):

$$ZnO + h\upsilon \rightarrow h^{+}_{VB} + e^{-}_{CB}$$

$$OH^{-}_{(ads)} + h^{+}_{VB} \rightarrow OH^{\bullet}_{(ads)}$$

$$H_2O + h^{+}_{VB} \rightarrow OH^{\bullet} + H^{+}$$

$$2OH^{\bullet} \rightarrow H_2O_2$$

$$2H^{+} + O_2 + 2e^{-}_{CB} \rightarrow H_2O_2$$

$$2H_2O + 2h^{+}_{VB} \rightarrow H_2O_2 + 2H^{+}$$

$$H_2O_2 + h\upsilon \rightarrow 2OH^{\bullet}$$

$$O_{2(ads)} + e^{-}_{CB} \rightarrow O^{\bullet}_{2}-$$

$$O_2^{-} + e^{-}_{CB} + 2H^{+} \rightarrow H_2O_2$$

$$O^{\bullet}_{2} - + H_2O_2 \rightarrow OH^{\bullet} + OH^{-} + O_2$$

$$O^{\bullet}_{2} - + H^{+} \rightarrow OOH^{\bullet}$$

$$O^{\bullet}_{2} - + h^{+}_{VB} \rightarrow {}^{1}O_2$$

$$OOH^{\bullet} + O^{\bullet -}_{2} + H^{+} \rightarrow O_2 + H_2O_2$$

$$(\text{tartrazine dye})_{ads} + h\upsilon \rightarrow (\text{tartrazine dye})^{*}_{ads}$$

$$(\text{tartrazine dye})^{*}_{ads} + ZnO \rightarrow (\text{tartrazine dye})^{\bullet +}_{ads} + ZnO(e^{-})$$

$$(\text{tartrazine dye})^{*}_{ads} + O_2 \rightarrow (\text{tartrazine dye})_{ads} + {}^{1}O_2$$

$$(\text{tartrazine dye}) + ZnO\ (e-) \rightarrow (\text{tartrazine dye})^{\bullet -}$$

$$(\text{tartrazine dye}) + h^{+}_{VB} \rightarrow (\text{tartrazine dye})^{\bullet +}$$

Figure 13 demonstrates the mechanistic interpretation of the photocatalytic degradation reaction of tartrazine dye in the presence of photocatalyst ZnO under solar radiation onto the semiconductor.

For (Ce, Ag)/ZnO catalyst

The chemical reactions producing reactive chemical species mentioned above during the photocatalytic degradation of tartrazine by ZnO are also generated during the presence of (Ce, Ag) co-doped ZnO. In the case of (Ce, Ag)/ZnO catalyst, the improvement of photocatalysis in the presence of Ag and Ce has been presented as follows.

Figure 14 demonstrates the mechanistic interpretation of the photocatalytic reaction for the photocatalyst (Ce, Ag) co-doped ZnO. When solar radiation illuminates the semiconductor. The presence of Ag and Ce simultaneously traps the electron from the CB of ZnO which suppresses the recombination of the electron-hole. The photocatalytic process occurs in which oxygen adsorbed on the photocatalyst surface traps the photogenerated electron (Mills & McGrady 2008). The transition of the electron to oxygen can be the rate-determining step in the photocatalytic reaction of semiconductors (Mura *et al.* 2002). The role of Ag in the photocatalytic process of trapping the electrons from ZnO's CB during solar irradiation is reported in the literature (Chen & Nickel 1996). The doped Ag in the ZnO photocatalyst can function as an electron collector to increase the lifespan of charge carriers because the Fermi energy level of the noble metal (Ag) is still greater than that of the photocatalyst semiconductor (Zhang *et al.* 2013). Improvement of (Ce, Ag) co-doped ZnO photocatalytic reaction is due to a synergistic interaction between Ag and Ce in ZnO. Photocatalytic performance of (Ce, Ag) co-doped ZnO is found to be better than that of ZnO.

For the Ce-doped ZnO photocatalyst, the Ce^{4+} ions incorporated in the ZnO lattice are intended to absorb photo-excited electrons from the conduction band of ZnO

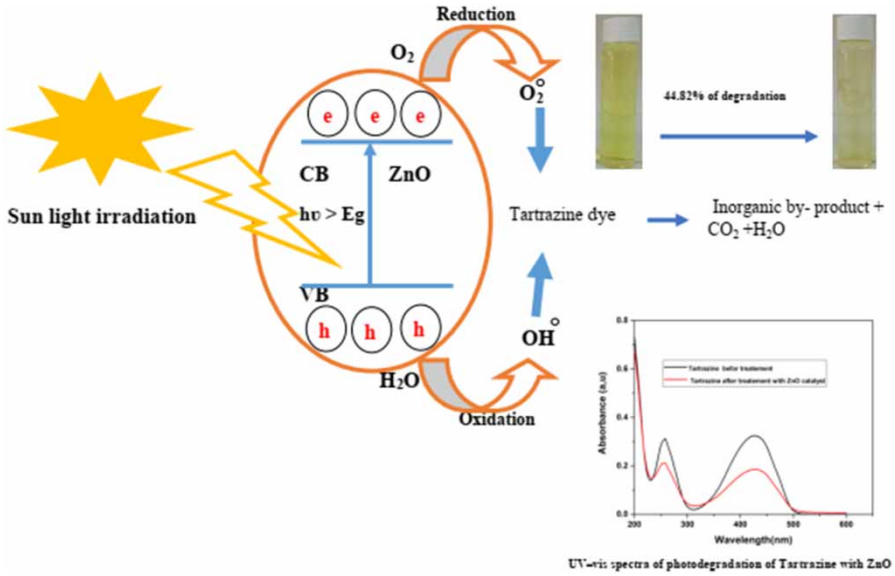

Figure 13 | Mechanism of degradation of tartrazine by ZnO.

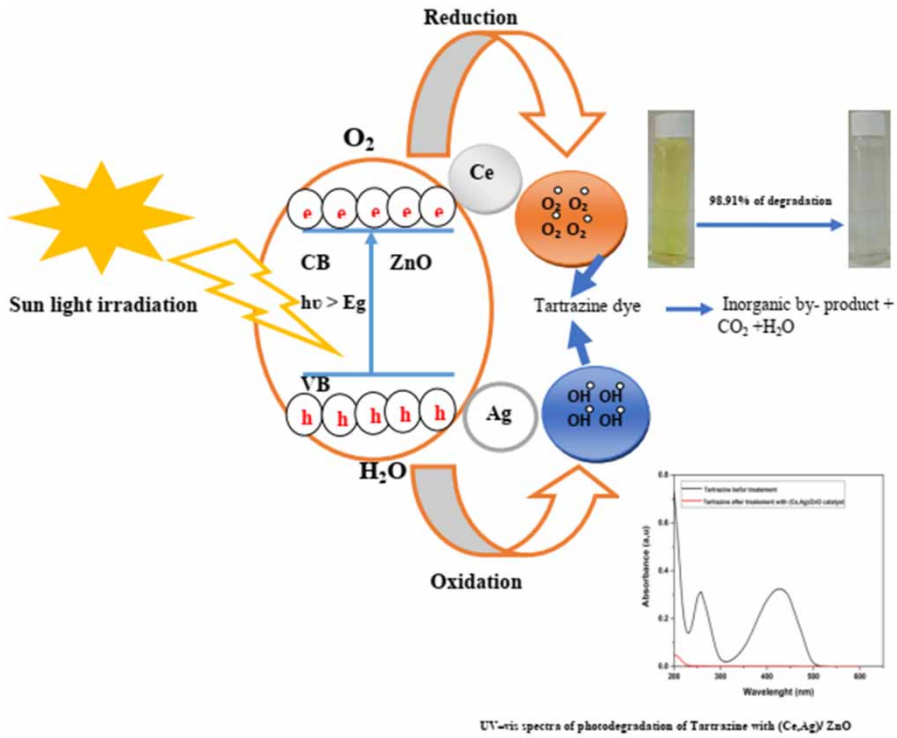

Figure 14 | Mechanism of degradation of tartrazine by (Ce, Ag)/ZnO.

and reduce them to Ce^{3+} ions. Reduced Ce^{3+} ions are oxidized by passing the electron to the adsorbed O_2 molecules, producing the radical superoxide ($O_2^{\prime -}$) (Coronado *et al.* 2002; Kannadasan *et al.* 2014; Kuzhalosai *et al.* 2014). However, Ce^{4+} readily catches the photo-excited electron in the Ce-doped ZnO catalyst. This is because Ce^{4+} is a Lewis acidic entity and is better at trapping electrons than the oxygen molecule (O_2) (Coronado *et al.* 2002). The electrons at Ce^{4+} sites are subsequently passed to the adsorbed O_2 by oxidation, which increases the simple

recombination of electrons and holes, as seen in the following:

$$Ce^{4+} + e^{-} \rightarrow Ce^{3+}$$

$$Ce^{3+} + O_2 \rightarrow O_2^{\bullet} + Ce^{4+}$$

It can also be shown that the Ce 4f level in (Ce, Ag) co-doped ZnO plays a significant role in the conversion and inhibition of electron-hole recombination of interfacial charges. The UV–Vis-spectrum reveals that Ag and Ce co-doping increases the visible light absorption of ZnO and produces more electron-hole pairs under solar light irradiation, which aims to enhance the photocatalytic function of the photocatalyst (Ce, Ag) co-doped ZnO.

Ce^{4+} quickly captures the electron, and it serves as an electron scavenger. The coexistence of Ce^{3+} and Ce^{4+} in (Ce, Ag) co-doped ZnO affect the photo-reactivity by altering the recombination of electron-hole pairs. In addition, the trapping aspect of Ag and Ce^{4+}/Ce^{3+} sites is consequently passed to the adjacent adsorbed O_2 to create a significant number of radical superoxide anions. At the same time, ZnO's VB holes react with water to generate highly reactive hydroxyl (OH^{-}) radical compounds. Dye oxidation is caused by the strongly reactive superoxide radical anion and hydroxyl radicals. The increase in the production of O_2 and OH by Ce and Ag increases the photocatalytic activity of (Ce, Ag)/ZnO (Subash *et al.* 2012).

CONCLUSION

With the synthesis of pure and (Ce, Ag) co-doped ZnO by solvothermal method, the presence of Ce and Ag co-doped ZnO has been revealed by XRD. The pure ZnO exhibited good photocatalytic activity with a degradation of 77.77% for tartrazine at pH = 9. The (Ce, Ag)/ZnO catalyst exhibited outstanding photocatalytic activity for the photodegradation of tartrazine under sunlight at different pH = 3, 6, and 9, and the different concentrations of the pollutant (10.20 mg/L and 30 mg/L). The improved photocatalytic output of (Ce, Ag)/ZnO could be due to the narrowing of ZnO band gap energy resulting from the efficient high charge separation. The (Ce, Ag)/ZnO catalyst was found to be highly efficient and recyclable and therefore reusable. The excellent photocatalytic properties of (Ce, Ag)/ZnO for degradation of tartrazine to the extent of 98.91% has been found within 90 min under solar irradiation. (Ce, Ag)/ZnO therefore has potential and can act as an efficient catalyst for the degradation of tartrazine.

ACKNOWLEDGEMENTS

The authors of this manuscript would like to thank the General Directorate for Scientific Research and Technological Development (DGRSDT) and the Ministry of Higher Education and Scientific Research (MESRS), Algeria, for funding this project. The authors would also like to thank Dr Fouzia Touahra, CRAPC, for his valuable input in the project.

DATA AVAILABILITY STATEMENT

All relevant data are included in the paper or its Supplementary Information.

REFERENCES

Abdullah Hashim, H. A., Mohamed, A. R. & Lee, K. T. 2001 Solar photocatalytic degradation of tartrazine using titanium dioxide. *Jurnal Teknologi* **35**, 31–40. https://doi.org/10.11113/jt.v35.618.

Ali, S. R., Kumar, R., Kadabinakatti, S. K. & Arya, M. C. 2018a Enhanced UV and visible light – driven photocatalytic degradation of tartrazine by nickel-doped cerium oxide nanoparticles. *Materials Research Express* **6**, 025513. https://doi.org/10.1088/2053-1591/aaee44.

Ali, S. R., Kumar, R., Kadabinakatti, S. K. & Arya, M. C. 2018b Enhanced UV and visible light – driven photocatalytic degradation of tartrazine by nickel-doped cerium oxide nanoparticles. *Materials Research Express* **6**, 025513. https://doi.org/10.1088/2053-1591/aaee44.

Ani, I. J., Akpan, U. G., Olutoye, M. A. & Hameed, B. H. 2018 Photocatalytic degradation of pollutants in petroleum refinery wastewater by TiO2- and ZnO-based photocatalysts: recent development. *Journal of Cleaner Production* **205**, 930–954. https://doi.org/10.1016/j.jclepro.2018.08.189.

Aoudjit, L., Madjene, F., Lebik, H., Boutra, B., Sebti, A. & Igoud, S. 2017 Photo degradation of CI Acid Yellow 23 using immobilized ZnO under sunlight irradiation. *Algerian Journal of Environment Science & Technology* **3**, 60–63.

Aoudjit, L., Martins, P. M., Madjene, F., Petrovykh, D. Y. & Lanceros-Mendez, S. 2018 Photocatalytic reusable membranes for the effective degradation of tartrazine with a solar photoreactor. *Journal of Hazardous Materials* **344**, 408–416. https://doi.org/10.1016/j.jhazmat.2017.10.053.

Aoudjit, F., Touahra, F., Aoudjit, L., Cherifi, O. & Halliche, D. 2020 Efficient solar hetero generous photocatalytic degradation of metronidazole using heterojunction

semiconductors hybrid nano composite layered double hydroxides. *Water Science and Technology* **82**, 2837–2846. https://doi.org/10.2166/wst.2020.519.

Baruah, S., Khan, M. N. & Dutta, J. 2015 Perspectives and applications of nanotechnology in water treatment. *Environmental Chemistry Letters* **14**, 1–14. https://doi.org/10.1007/s10311-015-0542-2.

Beura, R. & Thangadurai, P. 2017 Structural, optical and photocatalytic properties of graphene-ZnO nanocomposites for varied compositions. *Journal of Physics and Chemistry of Solids* **102**, 168–177. https://doi.org/10.1016/j.jpcs.2016.11.024.

Bhatt, D., Vyas, K., Singh, S., John, P. J., Bhatt, D., Vyas, K., Singh, S., John, P. J. & Inderpal, S. 2018 Tartrazine induced neurobiochemical alterations in rat brain sub-regions. *Food and Chemical Toxicology* **113**, 322–327. https://doi.org/10.1016/j.fct.2018.02.011.

Brillas, E. & Martínez-Huitle, C. A. 2015 Decontamination of wastewaters containing synthetic organic dyes by electrochemical methods. An updated review. *Applied Catalysis B: Environmental* **66**, 603–643. https://doi.org/10.1016/j.apcatb.2014.11.016.

Chang, C.-J., Lin, C.-Y. & Hsu, M.-H. 2014 Enhanced photocatalytic activity of Ce-doped ZnO nanorods under UV and visible light. *Journal of the Taiwan Institute of Chemical Engineers* **45**, 1954–1963. https://doi.org/10.1016/j.jtice.2014.03.008.

Chekir, N., Tassalit, D., Benhabiles, O., Merzouk, N. K., Ghenna, M., Abdessemed, A. & Issaadi, R. 2017 A comparative study of tartrazine degradation using UV and solar fixed bed reactors. *International Journal of Hydrogen Energy* **42**, 8948–8954. https://doi.org/10.1016/j.ijhydene.2016.11.057.

Chen, S. & Nickel, U. 1996 Controllable exciton bleaching and recovery observed in ZnO–Ag hybrid nanometre-sized particles. *Chemical Communications* 133–134. https://doi.org/10.1039/CC9960000133.

Chen, Y., Yang, S., Wang, K. & Lou, L. 2005 Role of primary active species and TiO2 surface characteristic in UV-illuminated photodegradation of Acid Orange 7. *Journal of Photochemistry and Photobiology A: Chemistry* **172**, 47–54. https://doi.org/10.1016/j.jphotochem.2004.11.006.

Chen, Y., Sun, F., Huang, Z., Chen, H., Zhuang, Z., Pan, Z., Long, J & Gu, F. 2017 Photochemical fabrication of SnO2 dense layers on reduced graphene oxide sheets for application in photocatalytic degradation of p -Nitrophenol. *Applied Catalysis B: Environmental* **215**, 8–17. https://doi.org/10.1016/j.apcatb.2017.03.082.

Coronado, J. M., Javier Maira, Arturo, A. J., Martínez-Arias, A., Conesa, J. C. C. & Soria, J. 2002 EPR study of the radicals formed upon UV irradiation of ceria-based photocatalysts. *Journal of Photochemistry and Photobiology A: Chemistry* **150**, 213–221. https://doi.org/10.1016/S1010-6030(02)00092-8.

Daneshvar, N., Rabbani, M., Modirshahla, N. & Behnajady, M. A. 2005 Photooxidative degradation of Acid Red 27 in a tubular continuous-flow photoreactor: influence of operational parameters and mineralization products. *Journal of Hazardous Materials* **118**, 155–160. https://doi.org/10.1016/j.jhazmat.2004.10.007.

Davis, R. J., Gainer, J. L., O'Neal, G. & Wu, I.-W. 1994 Photocatalytic decolorization of wastewater dyes. *Water Environment Research* **66**, 50–53. https://doi.org/10.2175/WER.66.1.8.

Dong, S., Li, Y., Sun, J., Yu, C., Li, Y. & Sun, J. 2014 Facile synthesis of novel ZnO/RGO hybrid nanocomposites with enhanced catalytic performance for visible-light-driven photodegradation of metronidazole. *Materials Chemistry and Physics* **145**, 357–365. https://doi.org/10.1016/j.matchemphys.2014.02.024.

dos Santos, T. C., Zocolo, G. J., Morales, D. A., de Aragão Umbuzeiro, G. & Zanoni, M. V. B. 2014 Assessment of the breakdown products of solar/UV induced photolytic degradation of food dye tartrazine. *Food and Chemical Toxicology* **68**, 307–315. https://doi.org/10.1016/j.fct.2014.03.025.

Farzadkia, M., Esrafili, A., Baghapour, M., Shahamat, Y. D. & Okhovat, N. 2014 Degradation of metronidazole in aqueous solution by nano-ZnO/UV photocatalytic process. *Desalination and Water Treatment* **52**, 4947–4952. https://doi.org/10.1080/19443994.2013.810322.

Fu, Y., Huang, T., Zhang, L., Zhu, J. & Wang, X. 2015 Ag/g-C_3N_4 catalyst with superior catalytic performance for the degradation of dyes: a borohydride-generated superoxide radical approach. *Nanoscale* **7**, 13723–13733. https://doi.org/10.1039/C5NR03260A.

Fujishima, A., Zhang, X. & Tryk, D. 2008 TiO2 photocatalysis and related surface phenomena. *Surface Science Reports* **63**, 515–582. https://doi.org/10.1016/j.surfrep.2008.10.001.

Ghribi, F., Sehailia, M., Aoudjit, L., Touahra, F., Zioui, D., Boumechhour, A., Halliche, D., Bachari, K. & Benmaamar, Z. 2020 Solar-light promoted photodegradation of metronidazole over ZnO-$ZnAl_2O_4$ heterojunction derived from 2D-layered double hydroxide structure. *Journal of Photochemistry and Photobiology A: Chemistry* 112510. https://doi.org/10.1016/j.jphotochem.2020.112510

Guo, M. Y., Ng, A. M. C., Liu, F., Djurišić, A. B. & Chan, W. K. 2011 Photocatalytic activity of metal oxides – the role of holes and OH radicals. *Applied Catalysis B: Environmental* **107**, 150–157. https://doi.org/10.1016/j.apcatb.2011.07.008.

Güy, N. & Özacar, M. 2019 Ag/Ag2CrO4 nanoparticles modified on ZnO nanorods as an efficient plasmonic photocatalyst under visible light. *Journal of Photochemistry and Photobiology A: Chemistry* **370**, 1–11. https://doi.org/10.1016/j.jphotochem.2018.10.035.

Habba, Y. G., Capochichi-Gnambodoe, M., Serairi, L. & Leprince-Wang, Y. 2016 Enhanced photocatalytic activity of ZnO nanostructure for water purification: enhanced photocatalytic activity of ZnO nanostructure. *Physica Status Solidi B Basic Solid State Physics* **253**, 1480–1484. https://doi.org/10.1002/pssb.201600031.

Herrmann, J. M., Guillard, C. & Pichat, P. 1993 Heterogeneous photocatalysis: An emerging technology for water treatment. *Catalysis Today* **17**, 7–20. https://doi.org/10.1016/0920-5861(93)80003-J.

Igoud, S., Zeriri, D., Aoudjit, L., Boutra, B., Sebti, A., Khene, F. & Mameche, A. 2020 Climate change adaptation by solar

wastewater treatment (SOWAT) for reuse in agriculture and industry. *Irrigation and Drainage* ird.2540. https://doi.org/10.1002/ird.2540.

Jamil, T. S. & Sharaf El-Deen, S. E. A. 2016 Removal of persistent tartrazine dye by photodegradation on TiO_2 nanoparticles enhanced by immobilized calcinated sewage sludge under visible light. *Separation Science and Technology* **51**, 1744–1756. https://doi.org/10.1080/01496395.2016.1170036.

Kamegawa, T., Suzuki, N. & Yamashita, H. 2011 Design of macroporous TiO2 thin film photocatalysts with enhanced photofunctional properties. *Energy & Environmental Science* **4**, 1411. https://doi.org/10.1039/c0ee00389a.

Kamegawa, T., Seto, H., Matsuura, S. & Yamashita, H. 2012 Preparation of hydroxynaphthalene-modified TiO $_2$ via formation of surface complexes and their applications in the photocatalytic reduction of nitrobenzene under visible-light irradiation. *ACS Applied Materials & Interfaces* **4**, 6635–6639. https://doi.org/10.1021/am3017762.

Kannadasan, N., Shanmugam, N., Cholan, S., Sathishkumar, K., Viruthagiri, G. & Poonguzhali, R. 2014 The effect of Ce4+ incorporation on structural, morphological and photocatalytic characters of ZnO nanoparticles. *Materials Characterization* **97**, 37–46. https://doi.org/10.1016/j.matchar.2014.08.021.

Kao, C.-Y., Liao, J.-D., Chang, C.-W. & Wang, R.-Y. 2011 Thermal diffusion of Co into sputtered ZnO:Co thin film for enhancing visible-light-induced photo-catalytic activity. *Applied Surface Science* **258**, 1813–1818. https://doi.org/10.1016/j.apsusc.2011.10.050.

Kaur, J. & Singhal, S. 2014 Facile synthesis of ZnO and transition metal doped ZnO nanoparticles for the photocatalytic degradation of Methyl Orange. *Ceramics International* **40**, 7417–7424. https://doi.org/10.1016/j.ceramint.2013.12.088.

Khalid, N. R., Hammad, A., Tahir, M. B., Rafique, M., Iqbal, T., Nabi, G. & Hussain, M. K. 2019 Enhanced photocatalytic activity of Al and Fe co-doped ZnO nanorods for methylene blue degradation. *Ceramics International* **45**, 21430–21435. https://doi.org/10.1016/j.ceramint.2019.07.132.

Khatamian, M., Khandar, A. A., Divband, B., Haghighi, M. & Ebrahimiasl, S. 2012 Heterogeneous photocatalytic degradation of 4-nitrophenol in aqueous suspension by Ln (La3 + , Nd3+ or Sm3+) doped ZnO nanoparticles. *Journal of Molecular Catalysis A: Chemical* **365**, 120–127. https://doi.org/10.1016/j.molcata.2012.08.018.

Krishnakumar, B., Subash, B. & Swaminathan, M. 2012 Agbr–ZnO – an efficient nano-photocatalyst for the mineralization of Acid Black 1 with UV light. *Separation and Purification Technology* **85**, 35–44. https://doi.org/10.1016/j.seppur.2011.09.037.

Kumar, R., Umar, A., Kumar, G., Akhtar, M. S., Wang, Y. & Kim, S. H. 2015 Ce-doped ZnO nanoparticles for efficient photocatalytic degradation of direct red-23 dye. *Ceramics International* **41**, 7773–7782. https://doi.org/10.1016/j.ceramint.2015.02.110.

Kumar, J. S., Bolimera, U. R. & Thangadurai, P. 2019 *Direct sunlight responsive ZnO photocatalyst: Highly efficient photodegradation of Methylene Blue*. Hisar, Haryana, India, p. 030080

Kumaran, N. N. & Muraleedharan, K. 2017 Photocatalytic activity of ZnO and Sr 2+ doped ZnO nanoparticles. *Journal of Water Process Engineering* **17**, 264–270. https://doi.org/10.1016/j.jwpe.2017.04.014.

Kuzhalosai, V., Subash, B. & Shanthi, M. 2014 A novel sunshine active cerium loaded zinc oxide photocatalyst for the effective degradation of AR 27 dye. *Materials Science in Semiconductor Processing* **27**, 924–933. https://doi.org/10.1016/j.mssp.2014.08.046.

Lam, S.-M., Sin, J.-C., Abdullah, A. Z. & Mohamed, A. R. 2012 Degradation of wastewaters containing organic dyes photocatalysed by zinc oxide: a review. *Desalination and Water Treatment* **41**, 131–169. https://doi.org/10.1080/19443994.2012.664698.

Lamba, R., Umar, A., Mehta, S. K. & Kansal, S. K. 2015 Ceo2zno hexagonal nanodisks: efficient material for the degradation of direct blue 15 dye and its simulated dye bath effluent under solar light. *Journal of Alloys and Compounds* **620**, 67–73. https://doi.org/10.1016/j.jallcom.2014.09.101.

Li, G., Lv, L., Fan, H., Ma, J., Li, Y., Wan, Y. & Zhao, X. S. 2010 Effect of the agglomeration of TiO2 nanoparticles on their photocatalytic performance in the aqueous phase. *Journal of Colloid and Interface Science* **348**, 342–347. https://doi.org/10.1016/j.jcis.2010.04.045.

Li, W., Ma, S., Yang, G., Mao, Y., Luo, J., Cheng, L., Gengzang, D., Xu, X. & Yan, S. 2015 Preparation, characterization and gas sensing properties of pure and Ce doped ZnO hollow nanofibers. *Materials Letters* **138**, 188–191. https://doi.org/10.1016/j.matlet.2014.09.130.

Martins, P. M., Salazar, H., Aoudjit, L., Gonçalves, R., Zioui, D., Fidalgo-Marijuan, A., Costa, C.M., Ferdov, S. & Lanceros-Mendez, S. 2021 Crystal morphology control of synthetic giniite for enhanced photo-Fenton activity against the emerging pollutant metronidazole. *Chemosphere* **262**, 128300. https://doi.org/10.1016/j.chemosphere.2020.128300.

Mills, A. & McGrady, M. 2008 A study of new photocatalyst indicator inks. *Journal of Photochemistry and Photobiology A: Chemistry* **193**, 228–236. https://doi.org/10.1016/j.jphotochem.2007.06.029.

Mura, G. M., Ganadu, M. L., Lombardi, P., Lubinu, G., Branca, M. & Maida, V. 2002 A preliminary comparison between hydrogenase and oxygen as electron acceptors in irradiated aqueous dispersion of titanium dioxide. *Journal of Photochemistry and Photobiology A: Chemistry* **148**, 199–204. https://doi.org/10.1016/S1010-6030(02)00043-6.

Nair, M. G., Nirmala, M., Rekha, K. & Anukaliani, A. 2011 Structural, optical, photo catalytic and antibacterial activity of ZnO and Co doped ZnO nanoparticles. *Materials Letters* **65**, 1797–1800. https://doi.org/10.1016/j.matlet.2011.03.079.

Nezamzadeh-Ejhieh, A. & Hushmandrad, S. 2010 Solar photodecolorization of methylene blue by CuO/X zeolite as a heterogeneous catalyst. *Applied Catalysis A: General* **388**, 149–159. https://doi.org/10.1016/j.apcata.2010.08.042.

Oller, I., Malato, S. & Sánchez-Pérez, J. A. 2011 Combination of advanced oxidation processes and biological treatments for wastewater decontamination: A review. *Science of the Total*

Environment **409**, 4141–4166. https://doi.org/10.1016/j.scitotenv.2010.08.061.

Omrani, N. & Nezamzadeh-Ejhieh, A. 2020 A comprehensive study on the enhanced photocatalytic activity of Cu_2O/$BiVO_4$/WO_3 nanoparticles. *Journal of Photochemistry and Photobiology A: Chemistry* **389**, 112223. https://doi.org/10.1016/j.jphotochem.2019.112223.

Poongodi, G., Kumar, R. M. & Jayavel, R. 2015 Structural, optical and visible light photocatalytic properties of nanocrystalline Nd doped ZnO thin films prepared by spin coating method. *Ceramics International* **41**, 4169–4175. https://doi.org/10.1016/j.ceramint.2014.12.098.

Rehman, K., Ashraf, A., Azam, F. & Akash, M. S. H. 2019 Effect of food azo-dye tartrazine on physiological functions of pancreas and glucose homeostasis. *Turkish Journal of Biochemistry* **44**, 197–206. https://doi.org/10.1515/tjb-2017-0296.

Rezaei, M. & Habibi-Yangjeh, A. 2013 Microwave-assisted preparation of Ce-doped ZnO nanostructures as an efficient photocatalyst. *Materials Letters* **110**, 53–56. https://doi.org/10.1016/j.matlet.2013.07.120.

Saien, J. & Soleymani, A. R. 2007 Degradation and mineralization of Direct Blue 71 in a circulating upflow reactor by UV/TiO_2 process and employing a new method in kinetic study. *Journal of Hazardous Materials* **144**, 506–512. https://doi.org/10.1016/j.jhazmat.2006.10.065.

Salt, D. E., Smith, R. D. & Raskin, I. 1998 Phytoremediation. *Annual Review of Plant Physiology and Plant Molecular Biology* **49**, 643–668. https://doi.org/10.1146/annurev.arplant.49.1.643

Salthammer, T., Mentese, S. & Marutzky, R. 2010 Formaldehyde in the indoor environment. *Chemical Reviews* **110**, 2536–2572. https://doi.org/10.1021/cr800399 g.

Saravanan, R., Karthikeyan, N., Gupta, V. K., Thirumal, E., Thangadurai, P., Narayanan, V. & Stephen, A. 2013 Zno/Ag nanocomposite: an efficient catalyst for degradation studies of textile effluents under visible light. *Materials Science and Engineering: C* **33**, 2235–2244. https://doi.org/10.1016/j.msec.2013.01.046.

Su, Y., Zhao, X., Bi, Y. & Han, X. 2019 ZnO/Ag–Ag2O microstructures for high-performance photocatalytic degradation of organic pollutants. *Clean Technologies and Environmental Policy* **21**, 367–378. https://doi.org/10.1007/s10098-018-1641-0.

Subash, B., Krishnakumar, B., Velmurugan, R., Swaminathan, M. & Shanthi, M. 2012 Synthesis of Ce co-doped Ag–ZnO photocatalyst with excellent performance for NBB dye degradation under natural sunlight illumination. *Catalysis Science & Technology* **2**, 2319. https://doi.org/10.1039/c2cy20254a.

Subash, B., Krishnakumar, B., Swaminathan, M. & Shanthi, M. 2013 Solar-light-assisted photocatalytic degradation of NBB dye on Zr-codoped Ag–ZnO catalyst. *Research on Chemical Intermediates* **39**, 3181–3197. https://doi.org/10.1007/s11164-012-0831-3.

Tanaka, K., Padermpole, K. & Hisanaga, T. 2000 Photocatalytic degradation of commercial azodyes. *Water Research* **34**, 327–333. https://doi.org/10.1016/S0043-1354(99)00093-7.

Tassalit, D., Lebouachera, S., Dechir, S., Chekir, N., Benhabiles, O. & Bentahar, F. 2016 Comparison between TiO2 and ZnO photocatalytic efficiency for the degradation of tartrazine contaminant in water. *International Journal of Environmental Science* **1**, 357–364.

Tran, N. H., Reinhard, M. & Gin, K. Y.-H. 2018 Occurrence and fate of emerging contaminants in municipal wastewater treatment plants from different geographical regions-a review. *Water Research* **133**, 182–207. https://doi.org/10.1016/j.watres.2017.12.029.

Tunesi, S. & Anderson, M. 1991 Influence of chemisorption on the photodecomposition of salicylic acid and related compounds using suspended titania ceramic membranes. *Journal of Physical Chemistry* **95**, 3399–3405. https://doi.org/10.1021/j100161a078.

Ullah, R. & Dutta, J. 2008 Photocatalytic degradation of organic dyes with manganese-doped ZnO nanoparticles. *Journal of Hazardous Materials* **156**, 194–200. https://doi.org/10.1016/j.jhazmat.2007.12.033.

Vaiano, V., Iervolino, G., Sannino, D., Murcia, J. J., Hidalgo, M. C., Ciambelli, P. & Navío, J. A. 2016 Photocatalytic removal of patent blue V dye on Au-TiO 2 and Pt-TiO 2 catalysts. *Applied Catalysis B: Environmental* **188**, 134–146. https://doi.org/10.1016/j.apcatb.2016.02.001.

Velmurugan, R. & Swaminathan, M. 2011 An efficient nanostructured ZnO for dye sensitized degradation of Reactive Red 120 dye under solar light. *Solar Energy Materials and Solar Cells* **95**, 942–950. https://doi.org/10.1016/j.solmat.2010.11.029.

Vieira, R. H. & Volesky, B. 2000 Biosorption: A solution to pollution? *International Microbiology* **3**, 17–24.

Wen, X.-J., Niu, C.-G., Zhang, L., Liang, C. & Zeng, G.-M. 2018 A novel Ag2O/CeO2 heterojunction photocatalysts for photocatalytic degradation of enrofloxacin: possible degradation pathways, mineralization activity and an in depth mechanism insight. *Applied Catalysis B: Environmental* **221**, 701–714. https://doi.org/10.1016/j.apcatb.2017.09.060.

Zhang, J., Wang, W. & Liu, X. 2013 Ag–ZnO hybrid nanopyramids for high visible-light photocatalytic hydrogen production performance. *Materials Letters* **110**, 204–207. https://doi.org/10.1016/j.matlet.2013.07.113.

Zhao, J., Wu, T., Wu, K., Oikawa, K., Hidaka, H. & Serpone, N. 1998 Photoassisted degradation of dye pollutants. 3. degradation of the cationic dye Rhodamine B in aqueous anionic surfactant/TiO_2 dispersions under visible light irradiation: evidence for the need of substrate adsorption on TiO_2 particles. *Environmental Science & Technology* **32**, 2394–2400. https://doi.org/10.1021/es9707926.

Zhao, N., Yao, M., Li, F. & Lou, F. 2011 Microstructures and photocatalytic properties of Ag+ and La3+ surface codoped TiO2 films prepared by sol–gel method. *Journal of Solid State Chemistry* **184**, 2770–2775. https://doi.org/10.1016/j.jssc.2011.08.014.

Zioui, D., Salazar, H., Aoudjit, L., Martins, P. M. & Lanceros-Méndez, S. 2019 Polymer-based membranes for oily wastewater remediation. *Polymers* **12**, 42. https://doi.org/10.3390/polym12010042.

First received 27 December 2020; accepted in revised form 9 March 2021. Available online 26 March 2021